Inorganic Chemistry
Article

Inorg. Chem. **2011**, *50*, 1229–1241 **1229**
DOI: 10.1021/ic1015516

Synthesis, Structural, and Photophysical Investigation of Diimine Triscarbonyl Re(I) Tetrazolato Complexes.

Melissa V. Werrett,[†] Daniel Chartrand,[‡] Julian D. Gale,[†] Garry S. Hanan,[‡] Jonathan G. MacLellan,[§] Massimiliano Massi,*[,†] Sara Muzzioli,[∥] Paolo Raiteri,[†] Brian W. Skelton,[⊥] Morry Silberstein,[†] and Stefano Stagni[∥]

[†]*Department of Chemistry, Curtin University, GPO Box U1987, Perth, Western Australia 6845, Australia,* [‡]*Department of Chemistry, D-600 Université de Montréal, 2900 Edouard-Montpetit Montréal, Quebec, Canada,* [§]*School of Chemistry, Monash University, Box 23, Clayton 3800, Victoria, Australia,* [∥]*Department of Physical and Inorganic Chemistry, University of Bologna, Viale Risorgimento 4, 40126 Bologna, Italy, and* [⊥]*School of Biomedical, Biomolecular and Chemical Sciences, The University of Western Australia, Stirling Highway, Crawley, Western Australia 6009, Australia*

Received August 2, 2010

The synthesis, structural, and photophysical properties of a novel family of neutral *fac*-[Re(**N^N**)(CO)$_3$(**L**)] complexes, where **N^N** is either 2,2′-bipyridine or 1,10-phenanthroline and **L** is a *para* functionalized 5-aryltetrazolate [namely, 5-phenyltetrazolate (**Tph**$^-$), 4-(tetrazolate-5-yl)benzaldehyde (**Tbdz**$^-$), 5-(4-acetylphenyl)tetrazolate (**Tacy**$^-$), and methyl 4-(tetrazolate-5-yl)benzoate (**Tmeb**$^-$)] are reported. The complexes were prepared by direct addition of the corresponding tetrazolate anion to the acetonitrile solvated *fac*-[Re(**N^N**)(CO)$_3$]$^+$ precursor. NMR data demonstrate that the coordination of the metal fragment is regiospecific at the N2 atom of the tetrazolate ring. These conclusions are also supported by X-ray structural determinations. Photophysical data were obtained in diluted and deaerated dichloromethane solutions displaying broad and structureless profiles with emission maxima ranging from 566 to 578 nm. The absorption profiles indicate the presence of higher energy intraligand (IL) $\pi-\pi^*$ transitions and lower energies ligand-to-ligand charge transfer (LLCT) and metal-to-ligand charge transfer (MLCT). As the last two transitions are mixed, they are better described as a metal-ligand-to-ligand charge transfer (MLLCT), a result that is also supported by density functional theory (DFT) calculations. The complexes show excited state lifetime values ranging from 102 to 955 ns, with associated quantum yield between 0.012 and 0.099. Compared to the parent neutral chloro or bromo [Re(**N^N**)(CO)$_3$X], the complexes show a slightly improved performance because of the π accepting nature of the tetrazolato ligand. The metal-to-ligand backbonding is in fact depleting the Re center of electron density, thus widening the HOMO−LUMO gap and reducing the non-radiative decay mechanism in accordance with the energy gap law. Finally, the electron-withdrawing or donating nature of the substituent on the phenyltetrazolato ligand allows the fine-tuning of the photophysical properties.

Introduction

The synthesis and photophysical investigation of *n*d^6 metal complexes,[1] such as those of Re(I),[2] Ru(II),[3] Os(II),[4] and Ir(III),[5] is still a very active area of research. When coupled with appropriately conjugated ligands (e.g., with an accessible π^* system such as polypyridines),[6,7] these complexes exhibit luminescence properties generally arising from their triplet metal-to-ligand charge transfer (^{3}MLCT) excited states.[8] The possibility of fine-tuning both the chemical and the photophysical properties of these compounds has made them extremely attractive from an applicative point of view in a variety of areas such as the fabrication of organic light emitting devices (OLEDs),[9] light emitting electrochemical cells (LEECs),[10] and solar cells.[11,12] Moreover, the phosphorescent nature of their emission (triplet to singlet radiative decay) is

*To whom correspondence should be addressed. E-mail: m.massi@curtin.edu.au. Phone: +61-8-92662838. Fax: +61-8-9266-2300.

(1) Balzani, V.; Bergamini, G.; Campagna, S.; Puntoriero, F. *Top. Curr. Chem.* **2007**, *280*, 1.
(2) Kirgan, R. A.; Sullivan, B. P.; Rillema, D. P. *Top. Curr. Chem.* **2007**, *281*, 45.
(3) Campagna, S.; Puntoriero, F.; Nastasi, F.; Bergamini, G.; Balzani, V. *Top. Curr. Chem.* **2007**, *280*, 117.
(4) Kumaresan, D.; Shankar, K.; Vaidya, S.; Schmehl, R. H. *Top. Curr. Chem.* **2007**, *281*, 101.
(5) Flamigni, L.; Barbieri, A.; Sabatini, C.; Ventura, B.; Barigelletti, F. *Top. Curr. Chem.* **2007**, *281*, 143.
(6) Accorsi, G.; Listorti, A.; Yoosaf, K.; Armaroli, N. *Chem. Soc. Rev.* **2009**, *38*, 1690.
(7) Medlycott, E. A.; Hanan, G. S. *Chem. Soc. Rev.* **2005**, *34*, 133.
(8) Lakowicz, J. R. *Principles of Fluorescence Spectroscopy*, 2nd ed.; Kluwer Academic: New York, 1999.
(9) Holder, E.; Langeveld, B. M. W.; Schubert, U. S. *Adv. Mater.* **2005**, *17*, 1109.

Published on Web 01/26/2011

characterized by large Stokes shifts and longer excited state lifetimes (τ). These properties, which help in preventing self-quenching and reducing autofluorescence in biological tissues with the use of time-gated spectroscopy, also make luminescent nd^6 complexes promising candidates for novel biological markers and in immunoassays.[13−16]

The most popular Re(I) family of complexes studied for their luminescent properties is the *fac*-[Re(**N^N**)(CO)$_3$(**L**)]$^{n+}$,[2,17−22] where **N^N** represents a neutral conjugated diimine ligand such as 2,2′-bipyridine (**bipy**) or 1,10-phenanthroline (**phen**), **L** is an ancillary ligand, and n = 0 or 1 depending on the respective anionic or neutral charge of the **L** ligand. Some of these complexes exhibit exceptional luminescence properties with quantum yield (Φ) values up to 0.6 and extended excited state lifetimes τ ranging from the nano- to microsecond scale.[2] Manipulation of the photophysical properties is achieved by changing the relative energy of the π^* orbitals of the diimine system with the introduction of electron withdrawing (EWGs) or donating groups (EDGs) and/or by varying the crystal field strength of the ancillary ligand **L**.[2,23−33] Generally, cationic *fac*-[Re(**N^N**)(CO)$_3$(**L**)]$^+$ complexes, for example, when **L** is a pyridine-type ligand, possess superior photoluminescence properties compared to their analogous neutral ones where **L** = Cl^-, Br^-.[2] These improved properties have been rationalized in terms of a reduced non-radiative decay constant, k_{nr}, due to the larger gap between the highest occupied molecular orbital (HOMO) and the lowest unoccupied molecular orbital (LUMO), in agreement with the energy gap law.[34]

Tetrazoles are considered the nitrogen-based heterocyclic surrogate of the carboxylic acid group, which stems from the fact that the two functional groups possess very similar pK_a values.[35] Tetrazole containing compounds have been extensively studied as carboxylic acid analogues for the design of pharmaceuticals, antifungal, antibacterial formulations, and also very recently as crystal growth modifiers.[36,37] The coordination chemistry of the tetrazolate anion has been the focus of numerous investigations involving the preparation of metal complexes and hybrid inorganic−organic bi- and tridimensional systems (MOFs).[38−43] The majority of the work in these areas has been carried out with transition metals and, more recently, also with lanthanoid elements.[44−48] The variety of structural features that have been discovered upon coordinating tetrazolate anions to metal complexes is mainly due to the versatility of the heterocycle itself, exposing four σ bonding lone pairs, an aromatic donor π system, and an accepting π^* level.[35,49] Also, the development of the synthetic methods for the synthesis of tetrazoles has made possible the use of a large number of substrates for the conversion of nitriles (R-CN) into the corresponding R-CN$_4$H derivatives.[50,51]

Surprisingly, the coordination chemistry of the tetrazolate anion with Re is almost virtually unexplored, with only one example reported by Szczepura et al. of linkage between 5-methyltetrazolate and a hexanuclear $Re_6Se_8^{2+}$ cluster core.[52] The compound was obtained by addition of N_3^- with a coordinated molecule of acetonitrile, and no direct reaction of the tetrazole anion with Re precursors has been described to date. With the aim to expand the chemistry of Re tetrazolato complexes, we have prepared a series of compounds where the tetrazolato ligand is coordinated to the Re(**N^N**)(CO)$_3^+$

(10) Graber, S.; Doyle, K.; Neuburger, M.; Housecroft, C. E.; Constable, E. C.; Costa, R. D.; Orti, E.; Repetto, D.; Bolink, H. J. *J. Am. Chem. Soc.* **2008**, *130*, 14944.
(11) Polo, A. S.; Itokazu, M. K.; Iha, N. Y. M. *Coord. Chem. Rev.* **2004**, *248*, 1343.
(12) Spitler, M. T.; Parkinson, B. A. *Acc. Chem. Res.* **2009**, *42*, 2017.
(13) Fernandez-Moreira, V.; Thorp-Greenwood, F. L.; Coogan, M. P. *Chem. Commun.* **2010**, *46*, 186.
(14) Lo, K. K. W.; Louie, M. W.; Sze, K. S.; Lau, J. S. Y. *Inorg. Chem.* **2008**, *47*, 602.
(15) Amoroso, A. J.; Arthur, R. J.; Coogan, M. P.; Court, J. B.; Fernandez-Moreira, V.; Hayes, A. J.; Lloyd, D.; Millet, C.; Pope, S. J. A. *New J. Chem.* **2008**, *32*, 1097.
(16) Lo, K. K. W. *Top. Organomet. Chem.* **2010**, *29*, 115.
(17) Coleman, A.; Brennan, C.; Vos, J. G.; Pryce, M. T. *Coord. Chem. Rev.* **2008**, *252*, 2585.
(18) Worl, L. A.; Duesing, R.; Chen, P. Y.; Dellaciana, L.; Meyer, T. J. *J. Chem. Soc., Dalton Trans.* **1991**, 849.
(19) Vogler, A.; Kunkely, H. *Coord. Chem. Rev.* **2000**, *200*, 991.
(20) Striplin, D. R.; Crosby, G. A. *Chem. Phys. Lett.* **1994**, *221*, 426.
(21) Sacksteder, L.; Zipp, A. P.; Brown, E. A.; Streich, J.; Demas, J. N.; Degraff, B. A. *Inorg. Chem.* **1990**, *29*, 4335.
(22) Wrighton, M.; Morse, D. L. *J. Am. Chem. Soc.* **1974**, *96*, 998.
(23) Villegas, J. M.; Stoyanov, S. R.; Huang, W.; Rillema, D. P. *Inorg. Chem.* **2005**, *44*, 2297.
(24) Villegas, J. M.; Stoyanov, S. R.; Huang, W.; Rillema, D. P. *Dalton Trans.* **2005**, 1042.
(25) Czerwieniec, R.; Kapturkiewicz, A.; Lipkowski, J.; Nowacki, J. *Inorg. Chim. Acta* **2005**, *358*, 2701.
(26) Pornestchenko, I. E.; Polyansky, D. E.; Castellano, F. N. *Inorg. Chem.* **2005**, *44*, 3412.
(27) Horvath, R.; Otter, C. A.; Gordon, K. C.; Brodie, A. M.; Ainscough, E. W. *Inorg. Chem.* **2010**, *49*, 4073.
(28) Donghi, D.; D'Alfonso, G.; Mauro, M.; Panigati, M.; Mercandelli, P.; Sironi, A.; Mussini, P.; D'Alfonso, L. *Inorg. Chem.* **2008**, *47*, 4243.
(29) Chen, X. Y.; Femia, F. J.; Babich, J. W.; Zubieta, J. *Inorg. Chim. Acta* **2001**, *314*, 91.
(30) Mak, C. S. K.; Cheung, W. K.; Leung, Q. Y.; Chan, W. K. *Macromol. Rapid Commun.* **2010**, *31*, 875.
(31) Xue, W. M.; Chan, M. C. W.; Su, Z. M.; Cheung, K. K.; Liu, S. T.; Che, C. M. *Organometallics* **1998**, *17*, 1622.
(32) Cattaneo, M.; Fagalde, F.; Katz, N. E. *Inorg. Chem.* **2006**, *45*, 6884.
(33) Fraser, M. G.; Blackman, A. G.; Irwin, G. I. S.; Easton, C. P.; Gordon, K. C. *Inorg. Chem.* **2010**, *49*, 5180.
(34) Caspar, J. V.; Meyer, T. J. *J. Phys. Chem.* **1983**, *87*, 952.
(35) Butler, R. N. *Comprehensive Heterocyclic Chemistry II*; Pergamon Press: Oxford, 1996; Vol. *4*.
(36) Herr, R. J. *Bioorg. Med. Chem.* **2002**, *10*, 3379.
(37) Massi, M.; Ogden, M. I.; Radomirovic, T.; Jones, F. *CrystEngComm* **2010**, *12*, 4205.
(38) Lin, P.; Clegg, W.; Harrington, R. W.; Henderson, R. A. *Dalton Trans.* **2005**, 2388.
(39) Stagni, S.; Colella, S.; Palazzi, A.; Valenti, G.; Zacchini, S.; Paolucci, F.; Marcaccio, M.; Albuquerque, R. Q.; De Cola, L. *Inorg. Chem.* **2008**, *47*, 10509.
(40) Stagni, S.; Orselli, E.; Palazzi, A.; De Cola, L.; Zacchini, S.; Femoni, C.; Marcaccio, M.; Paolucci, F.; Zanarini, S. *Inorg. Chem.* **2007**, *46*, 9126.
(41) Stagni, S.; Palazzi, A.; Zacchini, S.; Ballarin, B.; Bruno, C.; Marcaccio, M.; Paolucci, F.; Monari, M.; Carano, M.; Bard, A. J. *Inorg. Chem.* **2006**, *45*, 695.
(42) Maspero, A.; Galli, S.; Colombo, V.; Peli, G.; Masciocchi, N.; Stagni, S.; Barea, E.; Navarro, J. A. R. *Inorg. Chim. Acta* **2009**, *362*, 4340.
(43) Duati, M.; Tasca, S.; Lynch, F. C.; Bohlen, H.; Vos, J. G.; Stagni, S.; Ward, M. D. *Inorg. Chem.* **2003**, *42*, 8377.
(44) Andreiadis, E. S.; Demadrille, R.; Imbert, D.; Pecaut, J.; Mazzanti, M. *Chem.—Eur. J.* **2009**, *15*, 9458.
(45) Andrews, P. C.; Junk, P. C.; Massi, M.; Silberstein, M. *Chem. Commun.* **2006**, 3317.
(46) Facchetti, A.; Abbotto, A.; Beverina, L.; Bradamante, S.; Mariani, P.; Stern, C. L.; Marks, T. J.; Vacca, A.; Pagani, G. A. *Chem. Commun.* **2004**, 1770.
(47) Giraud, M.; Andreiadis, E. S.; Fisyuk, A. S.; Demadrille, R.; Pecaut, J.; Imbert, D.; Mazzanti, M. *Inorg. Chem.* **2008**, *47*, 3952.
(48) Andrews, P. C.; Beck, T.; Fraser, B. H.; Junk, P. C.; Massi, M. *Polyhedron* **2007**, *26*, 5406.
(49) Palazzi, A.; Stagni, S.; Bordoni, S.; Monari, M.; Selva, S. *Organometallics* **2002**, *21*, 3774.
(50) Demko, Z. P.; Sharpless, K. B. *J. Org. Chem.* **2001**, *66*, 7945.
(51) Koguro, K.; Oga, T.; Mitsui, S.; Orita, R. *Synthesis* **1998**, 910.
(52) Szczepura, L. F.; Oh, M. K.; Knott, S. A. *Chem. Commun.* **2007**, 4617.

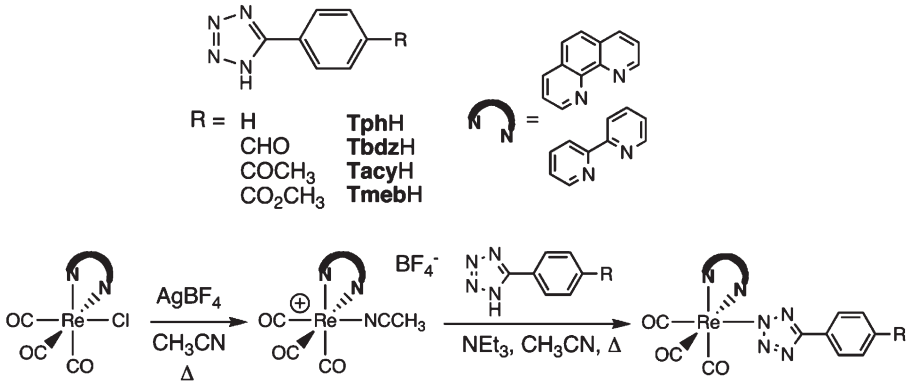

Figure 1. Synthetic pathway for the preparation of the Re tetrazolato complexes (the first reaction of $[Re(CO)_5Cl]$ with the diimine ligand **N^N** is not shown).

fragment, and have investigated their structural and photophysical properties using a variety of experimental and computational techniques. In this work, the investigated synthetic method involved the direct attachment of differently *para* substituted 5-aryltetrazolate anions to the acetonitrile solvated Re(I) precursor, as illustrated in Figure 1. The motivation that prompted us to undertake this study was the exploration of the luminescent properties of *fac*-[Re(**N^N**)$(CO)_3$(**L**)] complexes, where **L** represents a family of 5-aryltetrazolate ligands. While, in general, cationic triscarbonyl diimine Re(I) complexes have a better photophysical performance,[2] the advantage of neutral complexes lies in the possibility of device fabrication (e.g., OLEDs) by sublimation.[53] Devices obtained with this method have shown improved output efficiency. The tetrazole ligand, because of its σ donor and π acceptor nature, could be a promising candidate to improve the photo- and electroluminescent properties of neutral *fac*-[Re(**N^N**)$(CO)_3$(**L**)] compounds.

Experimental Section

General Considerations. All the reagents and solvents were obtained from Sigma Aldrich and used as received without any further purification, unless otherwise specified. Although not strictly required, all the reactions involving Re complexes were carried out under a nitrogen atmosphere following Schlenk protocols. When possible, the purification of the Re complexes was performed via column chromatography with the use of alumina as the stationary phase (Fluka, Brockmann activity I). IR spectra were recorded on solid samples using a diamond ATR Perkin-Elmer Spectrum 100 FT-IR. Nuclear magnetic resonance spectra (consisting of ^{1}H, ^{13}C, 1D NOE, HSQC, and HMBC experiments) were recorded using a Bruker Avance 400 spectrometer (400.1 MHz for ^{1}H, 100 MHz for ^{13}C) at room temperature. ^{1}H and ^{13}C chemical shifts were referenced to residual solvent resonances. Elemental analyses were performed by CMAS (Melbourne, Australia) on the desolvated bulk samples. Photophysical measurements were done in deoxygenated (by bubbling of argon gas) freshly distilled dichloromethane, using a borosilicate cell. Absorption and emission spectra were recorded at room temperature using a Cary 500i UV−Vis−NIR spectrophotometer and a Cary Eclipse 300 fluorimeter, respectively. The wavelengths for the emission and excitation spectra were determined using the absorption maxima of the metal-ligand-to-ligand charge transfer (MLLCT) transition bands (emission spectra) and at the maxima of the emission bands (excitation spectra). For quantum yields, an aerated solution of *fac*-[Re(**bipy**)$(CO)_3(NCCH_3)$][PF_6] was used as a reference, and its quantum yield (0.25) was measured with an Edinburgh Instruments FLS-920 fluorimeter equipped with an integrating sphere coated with barium sulfate. The remaining complexes were measured by the dilute solution method, with an excitation wavelength at 355 nm at constant absorption (0.26).[54] Lifetime measurements were done with an Edinburgh Instruments Mini Tau lifetime fluorimeter with an EPL 405 laser (exciting at 405 nm). Melting points were measured with a BI Barnsted Electrothermal 9100 apparatus and were quoted referencing the decomposition temperature.

Synthetic Methods. *fac*-[Re(**N^N**)$(CO)_3$Cl], *fac*-[Re(**N^N**)$(CO)_3(NCCH_3)$][BF_4] (**N^N** = **bipy** and **phen**),[55] **Tph**H,[51] **Tbdz**H,[51] **Tacy**H,[51] and **Tmeb**H[51] were prepared according to previously published procedures. *fac*-[Re(**N^N**)$(CO)_3(NCCH_3)$][BF_4] was treated as a reactive intermediate and was never isolated. *fac*-[Re(**N^N**)$(CO)_3(NCCH_3)$][BF_4] was dissolved in acetonitrile (30 mL). To this, an acetontrile solution containing 1.2 equiv of the corresponding tetrazole and 1.2 equiv of triethylamine was added. The resulting suspension was refluxed for 16 h and then filtered over Celite. The solvent was then reduced to approximately 5 mL, and the solution cooled in an ice bath, causing the precipitation of a yellow solid, which was filtered, washed with cold acetonitrile (2 × 5 mL), and dried under reduced pressure.

***fac*-[Re(bipy)$(CO)_3$(Tph)].** The *title compound* was purified via column chromatography using a 4:6 mixture CH_2Cl_2/CH_3CN as eluent (second fraction, yellow). Yield 0.113 g (44%). Mp 253 °C (dec.). Elemental analysis for $C_{20}H_{13}N_6O_3Re$: calcd: C 42.03, H 2.29, N 14.70; found: C 42.13, H 2.41, N 14.81. IR (ν, cm^{-1}): 3115 w, 3090 w, 3065 w, 3038 w, 2018 s (CO, A′(1)), 1893 s br (CO, A′(2)/A″), 1604 m (tetrazole CN), 1572 w, 1496 w, 1474 m, 1445 m, 1359 w, 1319 w, 1287 w, 1246 w, 1222 w, 1174 w, 1161 w, 1125 w, 1110 w, 1073 w, 1031 w, 1009 w, 971 w, 929 w, 899 w, 788 w, 767 m, 731 m, 690 m. ^{1}H NMR (δ, ppm, DMSO-d_6): 9.19 (2H, d, J = 5.6 Hz, bipy $H_{6,6'}$), 8.80 (2H, d, J = 8.2 Hz, bipy $H_{3,3'}$), 8.39 (2H, app. t, J = 7.2 Hz, bipy $H_{4,4'}$), 7.84−7.77 (2H, m, bipy $H_{5,5'}$), 7.67−7.65 (2H, m, $CN_4-C_6H_5$ H_o), 7.36−7.32 (3H, m, $CN_4-C_6H_5$ H_m, H_p). ^{13}C NMR (δ, ppm, DMSO-d_6): 197.9, 195.1, 162.3, 156.8, 154.4, 141.5, 130.3, 129,5, 129.3, 128.9, 126.5, 124.9.

***fac*-[Re(phen)$(CO)_3$(Tph)].** The *title compound* was purified via column chromatography using a 4:6 mixture CH_2Cl_2/CH_3CN as eluent (second fraction, yellow). Yield 0.104 g (42%). Mp 284 °C (dec.). Elemental analysis for $C_{22}H_{13}N_6O_3Re$: calcd: C 44.37, H 2.20, N 14.11; found: C 44.74, H 2.40, N

(53) Mauro, M.; Procopio, E. Q.; Sun, Y. H.; Chien, C. H.; Donghi, D.; Panigati, M.; Mercandelli, P.; Mussini, P.; D'Alfonso, G.; De Cola, L. *Adv. Funct. Mater.* **2009**, *19*, 2607.

(54) Crosby, G. A.; Demas, J. N. *J. Phys. Chem.* **1971**, *75*, 991.

(55) Amoroso, A. J.; Coogan, M. P.; Dunne, J. E.; Fernandez-Moreira, V.; Hess, J. B.; Hayes, A. J.; Lloyd, D.; Millet, C.; Pope, S. J. A.; Williams, C. *Chem. Commun.* **2007**, 3066.

14.23. IR (ν, cm^{-1}): 3092 w, 3067 w, 2019 s (CO, A′(1)), 1909 s (CO, A′(2)) 1884 s (CO, A″), 1631 w, 1605 w (tetrazole CN), 1585 w, 1519 m, 1496 w, 1459 w, 1426 m, 1362 w, 1347 w, 1313 w, 1280 w, 1225 w, 1147 w, 1126 w, 1112w, 1073 w, 1036 w, 1007 w, 998 w, 970 w, 930 w, 844 m, 788 w, 774 w, 733 m, 721 m, 692 m. ^{1}H NMR (δ, ppm, DMSO-d_6): 9.61 (2H, d, J = 5.2 Hz, phen $H_{2,9}$), 9.02 (2H, d, J = 8.0 Hz, phen $H_{4,7}$), 8.34 (2H, s, phen $H_{5,6}$), 8.19−8.12 (2H, m, phen $H_{3,8}$), 7.51−7.48 (2H, m, CN_4−C_6H_5 H_o), 7.26−7.24 (3H, m, CN_4−C_6H_5 H_m, H_p). ^{13}C NMR (δ, ppm, DMSO-d_6): 197.9, 194.6, 162.1, 155.2, 147.5, 140.7, 131.2, 130.1, 129.5, 129.4, 128.6, 127.6, 126.4.

***fac*-[Re(bipy)(CO)$_3$(Tbdz)].** The *title compound* was purified via filtration from hot acetonitrile. Yield 0.092 g (62%). Mp 265 °C (dec.). Elemental analysis for $C_{21}H_{13}N_6O_4Re$: calcd: C 42.07, H 2.19, N 14.02; found: C 42.00, H 2.26, N 14.07. IR (ν, cm^{-1}): 3067 w, 3059 w, 2823 w, 2731 w, 2021 s (CO, A′(1)), 1885 s br (CO, A′(2)/A″), 1696 m (aldehyde CO), 1603 m (tetrazole CN), 1573 w, 1531 w, 1494 w, 1470 m, 1446 m, 1388 w, 1312 w, 1302 w, 1281 w, 1265 w, 1244 w, 1205 m, 1159 w, 1119 w, 1103 w, 1071 w, 1037 w, 1004 w, 977 w, 833 m, 767 m, 756 m, 731 m, 693 w.

***fac*-[Re(phen)(CO)$_3$(Tbdz)].** The *title compound* was purified via column chromatography using a 4:6 mixture CH_2Cl_2/CH_3CN as eluent (second fraction, yellow). Yield 0.056 g (45%). Mp 268 °C (dec.). Elemental analysis for $C_{23}H_{13}N_6O_4Re$: calcd: C 44.30, H 2.10, N 13.48; found: C 44.02, H 2.23, N 13.21. IR (ν, cm^{-1}): 3107 w, 3069 w, 2020 s (CO, A′(1)), 1916 s (CO, A′(2)), 1892 s (CO, A″), 1697 (aldehyde CO), 1631 w, 1609 m (tetrazole CN), 1574 w, 1519 w, 1444 w, 1426 m, 1397 w, 1347 w, 1303 w, 1224 w, 1204 w, 1166 w, 1145 w, 1119 w, 1040 w, 1003 w, 854 w, 757 w, 722 w. ^{1}H NMR (δ, ppm, DMSO-d_6): 9.92 (1H, s, CN_4−C_6H_4−C*H*O), 9.59 (2H, d, J = 3.8 Hz, phen $H_{2,9}$), 8.99 (2H, d, J = 8.2 Hz, phen $H_{4,7}$), 8.31 (2H, s, phen $H_{5,6}$), 8.16−8.09 (2H, m, phen $H_{3,8}$), 7.82 (2H, d, J = 8.4 Hz, CN_4−C_6H_4−CHO H_m), 7.73 (2H, d, J = 8.3 Hz, CN_4−C_6H_4−CHO H_o). ^{13}C NMR (δ, ppm, DMSO-d_6): 197.7, 194.9, 193.3, 161.5, 155.2, 147.4, 140.7, 136.7, 135.4, 131.2, 130.9, 128.6, 127.6, 126.8.

***fac*-[Re(bipy)(CO)$_3$(Tacy)].** The *title compound* was purified via filtration from hot acetonitrile. Yield 0.052 g (30%). Mp 260 °C (dec.). Elemental analysis for $C_{22}H_{15}N_6O_4Re$: calcd: C 43.06, H 2.46, N 13.70; found: C 42.91, H 2.52, N 13.62. IR (ν, cm^{-1}): 3082 w, 3058 w, 3035 w, 2017 s (CO, A′(1)), 1898 s br (CO, A′(2)/A″), 1679 m (acetyl CO), 1604 m (tetrazole CN), 1570 w, 1530 w, 1497 w, 1475 m, 1445 w, 1418 w, 1359 w, 1320 w, 1301 w, 1283 w, 1254 m, 1175 w, 1161 w, 1123 w, 1108 w, 1076 w, 1038 w, 1006 w, 960 w, 913 w, 841 w, 776 m, 759 m, 730 m, 720 w, 662 w.

***fac*-[Re(phen)(CO)$_3$(Tacy)].** The *title compound* was purified via filtration from hot acetonitrile. Yield (bulk, not optimized) 0.029 g (22%). Mp 245 °C (dec.). Because of the very low solubility of the *title compound*, apart from in hot DMSO, purification of the bulk material proved particularly challenging. The bulk material was purified several times before an elemental analysis consistent with the formulation could be obtained. Elemental analysis for $C_{24}H_{15}N_6O_4Re$: calcd: C 45.21, H 2.37, N 13.18; found: C 45.52, H 2.43, N 13.25. IR (ν, cm^{-1}): 3046 w, 3006 w, 2016 s (CO, A′(1)), 1913 s (CO, A′(2)), 1887 (CO, A″), 1675 m (acetyl CO), 1630 w, 1612 m (tetrazole CN), 1585 w, 1572 w, 1531 w, 1519 w, 1427 m, 1359 w, 1300 w, 1285 w, 1263 m, 1226 w, 1175 w, 1159 w, 1147 w, 1123 w, 1107 w, 1040 m, 1024 w, 1006 w, 958 w, 847 m, 772 w, 758 w, 720 m.

***fac*-[Re(bipy)(CO)$_3$(Tmeb)].** The *title compound* was purified via filtration from hot acetonitrile. Yield 0.043 g (32%). Mp 275 °C (dec.). Elemental analysis for $C_{22}H_{15}N_6O_5Re$: calcd: C 41.97, H 2.40, N 13.35; found: C 42.05, H 2.53, N 13.49. IR (ν, cm^{-1}): 3075 w, 3035 w, 2949 w, 2020 s (CO, A′(1)), 1902 s br (CO, A′(2)/A″), 1721 s (ester CO), 1603 m (tetrazole CN), 1573 w, 1496 m, 1474 m, 1447 m, 1433 m, 1379 m, 1306 w, 1271 m, 1175 m, 1123 m, 1094 m, 1036 w, 1005 w, 863 w, 779 m, 740 m, 732 m, 694 w.

***fac*-[Re(phen)(CO)$_3$(Tmeb)].** The *title compound* was purified via filtration from hot acetonitrile. Yield 0.081 g (41%). Mp 243 °C (dec.). Elemental analysis for $C_{24}H_{15}N_6O_5Re$: calcd: C 44.10, H 2.31, N 12.86; found: C 44.19, H 2.58, N 13.07. IR (ν, cm^{-1}): 3049 w, 2957 w, 2020 s (CO, A′(1)), 1912 s (CO, A′(2)), 1887 (CO, A″), 1713 s (ester CO), 1678 w, 1615 m (tetrazole CN), 1584 w, 1534 w, 1519 wm 1449 w, 1427 m, 1307 w, 1277 m, 1226 w, 1212 w, 1190 w, 1174 w, 1150 w, 1141 w, 1108 w, 1098 w, 1037 w, 1005 w, 975 w, 864 w, 851 m, 829 w, 777 w, 737 m, 721 m, 698 m. ^{1}H NMR (δ, ppm, DMSO-d_6): 9.58 (2H, d, J = 4.0 Hz, phen $H_{2,9}$), 8.98 (2H, d, J = 7.4 Hz, phen $H_{4,7}$), 8.31 (2H, s, phen $H_{5,6}$), 8.16−8.09 (2H, m, phen $H_{3,8}$), 7.87 (2H, d, J = 8.4 Hz, CN_4−C_6H_4−CO_2CH_3 H_m), 7.66 (2H, d, J = 8.4 Hz, CN_4−C_6H_4−CO_2CH_3 H_o), 3.80 (3H, s, CO_2CH_3). ^{13}C NMR (δ, ppm, DMSO-d_6): 197.7, 196.4, 166.7, 161.5, 155.2, 147.3, 140.7, 134.3, 131.2, 130.5, 130.2, 128.6, 127.6, 126.5, 53.0.

X-ray Crystallography. Unless otherwise specified, diffraction data were collected at T = 100(2) K on an Oxford Diffraction Gemini diffractometer fitted with graphite-monochromated Mo Kα radiation (λ = 0.71073 Å). Following analytical absorption corrections and solution by direct methods, the structures were refined against F^2 with full-matrix least-squares using the program SHELXL-97.[56] All H-atoms were added at calculated positions and refined by use of riding models with isotropic displacement parameters based on those of the parent atoms. Anisotropic displacement parameters were employed throughout for the non-hydrogen atoms.

X-ray Crystal Data for *fac*-[Re(bipy)(CO)$_3$(Tph)]. Diffraction data were collected on a Bruker X8 Apex KAPPA CCD diffractometer fitted with graphite-monochromated Mo Kα X-ray radiation at 123(2) K and corrected for absorption using the SADABS package. Empirical formula $C_{20}H_{13}N_6O_3Re$; formula weight 571.56; crystal system: orthorhombic; space group *Pbca*; unit cell dimensions a = 11.5585(4), b = 9.2000(3), c = 35.8140(14) Å; volume 3808.4(2) $Å^3$; Z = 8; density (calculated) 1.994 Mg/m^3; absorption coefficient 6.418 mm^{-1}; F(000) 2192; crystal size 0.19 × 0.19 × 0.14 mm^3; θ range for data collection 2.10 to 27.87°; reflections collected 14294; independent reflections 4328 [R(int) = 0.1412]; completeness to θ = 25.00° 95.4%; data/restraints/parameters 4328/108/271; goodness-of-fit on F^2 0.998; final R indices [$I > 2\sigma(I)$] R_1 = 0.0656, wR_2 = 0.1210; R indices (all data) R_1 = 0.1750, wR_2 = 0.1593.

X-ray Crystal Data for *fac*-[Re(phen)(CO)$_3$(Tph)]. Empirical formula $C_{22}H_{13}N_6O_3Re$; formula weight 595.58; crystal system: triclinic; space group $P\bar{1}$; unit cell dimensions a = 9.2520(3), b = 9.3821(3), c = 12.9643(4) Å, α = 96.860(2), β = 105.448(3), γ = 110.008(3)°; volume 991.29(5) $Å^3$; Z = 2; density (calculated) 1.995 Mg/m^3; absorption coefficient 6.169 mm^{-1}; F(000) 572; crystal size 0.39 × 0.25 × 0.06 mm^3; θ range for data collection 3.83 to 40.36°; reflections collected 54643; independent reflections 12252 [R(int) = 0.0516]; completeness to θ = 40.00° 99.2%; data/restraints/parameters 12252/0/289; goodness-of-fit on F^2 1.003; final R indices [$I > 2\sigma(I)$] R_1 = 0.0370, wR_2 = 0.0873; R indices (all data) R_1 = 0.0461, wR_2 = 0.0901.

X-ray Crystal Data for *fac*-[Re(bipy)(CO)$_3$(Tbdz)]. Since the crystals were found to be invariably twinned, a number of samples were cleaved in attempts to obtain a suitable crystal. Also, since there appeared to be some crystal deterioration at lower temperatures, diffraction data were collected at 220(2) K. Empirical formula $C_{21}H_{13}N_6O_4Re$; formula weight 599.57 g/mol; crystal system: monoclinic; space group $P2_1/n$; unit cell dimensions a = 8.0117(2), b = 8.1105(3), c = 31.1788(10) Å, β = 94.702(2)°; volume 2019.15(11) $Å^3$; Z = 4; density (calculated) 1.972 Mg/m^3, absorption coefficient 6.061 mm^{-1}; F(000) 1152; crystal size 0.13 × 0.08 × 0.08 mm^3; θ range for data collection 3.58 to 27.50°; reflections collected 4684; independent reflections 4616 [R(int) = 0.053]; completeness to θ = 27.50° 99.0%;

(56) Sheldrick, G. M. *Acta Crystallogr.* **2008**, *A64*, 112.

data/restraints/parameters 4616/0/291; goodness-of-fit on F^2 1.183; final R indices [$I > 2\sigma(I)$] $R_1 = 0.0862$, $wR_2 = 0.1983$; R indices (all data) $R_1 = 0.0972$, $wR_2 = 0.2036$.

X-ray Crystal Data for *fac*-[Re(phen)(CO)$_3$(Tbdz)]. Empirical formula $C_{23}H_{13}N_6O_4Re$; formula weight 623.59 g/mol; crystal system: monoclinic; space group $P2_1/n$; unit cell dimensions a = 9.6886(5), b = 10.7874(3), c = 20.4181(18) Å, β = 95.615(7)°; volume 2123.8(2) Å^3; Z = 4; density (calculated) 1.950 Mg/m^3; absorption coefficient 5.767 mm^{-1}; F(000) 1200; crystal size 0.25 × 0.14 × 0.11 mm^3; θ range for data collection 3.55 to 34.96°; reflections collected 29861; independent reflections 8768 [R(int) = 0.0566]; completeness to θ = 34.00° 98.6%; data/restraints/parameters 8768/0/307; goodness-of-fit on F^2 0.786; final R indices [$I > 2\sigma(I)$] $R_1 = 0.0304$, $wR_2 = 0.0414$; R indices (all data) $R_1 = 0.0680$, $wR_2 = 0.0445$.

X-ray Crystal Data for *fac*-[Re(bipy)(CO)$_3$(Tacy)]. Empirical formula $C_{22}H_{15}N_6O_4Re$; formula weight 613.60 g/mol; crystal system: triclinic; space group $P\bar{1}$; unit cell dimensions a = 7.5265(2), b = 8.4382(2), c = 16.4431(4) Å, α = 98.986(2), β = 96.361(2), γ = 91.788(2)°; volume 1023.88(4) Å^3; Z = 2; density (calculated) 1.990 Mg/m^3; absorption coefficient 5.979 mm^{-1}; F(000) 592; crystal size 0.19 × 0.12 × 0.07 mm^3; θ range for data collection 3.73 to 36.39°; reflections collected 29744; independent reflections 9550 [R(int) = 0.0381]; completeness to θ = 35.50° 99.4%; data/restraints/parameters 9550/0/299; goodness-of-fit on F^2 0.968; final R indices [$I > 2\sigma(I)$] $R_1 = 0.0253$, $wR_2 = 0.0538$; R indices (all data) $R_1 = 0.0325$, $wR_2 = 0.0546$.

X-ray Crystal Data for *fac*-[Re(phen)(CO)$_3$(Tacy)]. Diffraction data were collected at 100(2) K on an Oxford Diffraction Xcalibur diffractometer fitted with graphite-monochromated Mo Kα radiation. Empirical formula $C_{24}H_{15}N_6O_4Re$; formula weight 637.62 g/mol; crystal system: monoclinic; space group $P2_1/n$; unit cell dimensions a = 7.46260(10), b = 17.8403(3), c = 16.7636(3) Å, β = 99.457(2)°; volume 2201.49(6) Å^3; Z = 4; density (calculated) 1.924 Mg/m^3; absorption coefficient 5.566 mm^{-1}; F(000) 1232; crystal size 0.17 × 0.15 × 0.05 mm^3; θ range for data collection 3.06 to 37.18°; reflections collected 79975; independent reflections 11100 [R(int) = 0.0461]; completeness to θ = 37.18° 98.0%; data/restraints/parameters 11100/0/317; goodness-of-fit on F^2 0.914; final R indices [$I > 2\sigma(I)$] $R_1 = 0.0236$, $wR_2 = 0.0438$; R indices (all data) $R_1 = 0.0427$, $wR_2 = 0.0461$.

X-ray Crystal Data for *fac*-[Re(bipy)(CO)$_3$(Tmeb)]. Empirical formula $C_{22}H_{15}N_6O_5Re$; formula weight 629.60 g/mol; crystal system: triclinic; space group $P\bar{1}$; unit cell dimensions a = 7.0089(2), b = 8.4369(2), c = 18.7123(4) Å, α = 102.980(2)°, β = 99.297(2)°, γ = 91.745(2)°; volume 1061.52(5) Å^3; Z = 2; density (calculated) 1.970 Mg/m^3; absorption coefficient 5.773 mm^{-1}; F(000) 608; crystal size 0.31 × 0.12 × 0.045 mm^3; θ range for data collection 3.72 to 41.06°; reflections collected 43713; independent reflections 13752 [R(int) = 0.0302]; completeness to θ = 40.50° 99.8%; data/restraints/parameters 13752/0/308; goodness-of-fit on F^2 0.917; final R indices [$I > 2\sigma(I)$] R_1 = 0.0193, $wR_2 = 0.0335$; R indices (all data) $R_1 = 0.0277$, wR_2 = 0.0342.

X-ray Crystal Data for *fac*-[Re(phen)(CO)$_3$(Tmeb)]. Empirical formula $C_{24}H_{15}N_6O_5Re$; formula weight 653.62 g/mol; crystal system: monoclinic; space group $P2_1/c$; unit cell dimensions a = 15.2843(4), b = 19.4828(4), c = 15.8578(3) Å, β = 102.071(3)°; volume 4617.74(18) Å^3; Z = 8; density (calculated) 1.88 Mg/m^3; absorption coefficient 5.313 mm^{-1}; F(000) 2528; crystal size 0.35 × 0.19 × 0.02 mm^3; θ range for data collection 3.77 to 30.0°; reflections collected 47138; independent reflections 13451 [R(int) = 0.0764]; completeness to θ = 30.00°, 99.8%; data/restraints/parameters 13451/0/651; goodness-of-fit on F^2 0.786; final R indices [$I > 2\sigma(I)$] $R_1 = 0.0406$, $wR_2 = 0.0685$; R indices (all data) $R_1 = 0.0920$, $wR_2 = 0.0743$.

Computational Methods: Solid-State. All solid-state quantum mechanical calculations have been performed within the Kohn−Sham density functional theory, as implemented within the SIESTA methodology[57] and package. Here the Generalized Gradient Approximation has been employed based on the AM05 exchange-correlation functional.[58] This functional has been found to yield improved geometries relative to many other GGA functionals, which typically show a systematic under binding, while being comparable to parametrizations that are explicit designed specifically for the solid-state.

Within the SIESTA methodology the core electrons and nuclei are represented through the use of norm-conserving pseudopotentials, and the modified Troullier-Martins form[59] has been used in the present work. Valence configurations consisting of the 2s and 2p orbitals were employed for C, N, and O, while for Re the 6s^{2}5d^2 electronic state was explicitly considered. A double-ζ polarized (DZP) basis set was employed for all elements except Re, for which no f polarization functions were included. A split-norm of 0.15 was used to create the second zeta for heavy elements, while a larger value of 0.5 was specified for hydrogen. The numerical basis functions were strictly confined within radii of 7 Bohr for all functions, except for those of Re (8 Bohr) and the explicit polarization function of H (3.5 Bohr). Soft confinement[60] was employed for all basis functions with a potential of 100 Ry and inner radius of 0.95 times the outer confinement value. In the case of the polarization functions the soft confinement parameters were modified such that the inner radii are zero and the potentials were 120 and 70 Ry for heavy atoms and hydrogen, respectively.

The electron density was expanded in an auxiliary basis set consisting of a Cartesian mesh with a fineness determined by the equivalent kinetic energy cutoff of 250 Ry. In addition, to minimize any breaking of translational invariance, grid cell sampling was employed based on averaging of the forces over two positions displaced by half the mesh spacing along each axis. For calculations on the crystallographic unit cell, integration across the Brillouin zone was performed using a Monkhorst−Pack mesh determined according to an equivalent real space cutoff of 12 Å. For supercell calculations simulating an isolated molecule only the Γ point was sampled. Full geometry optimization of the atomic coordinates was performed within the crystallographic unit cell using a tight convergence threshold of 0.002 eV/Å. A more stringent than usual tolerance was found to be necessary to ensure proper convergence of the torsional angles.

Computational Methods: Solution. To confirm the interpretation of the photophysical results we performed a series of molecular quantum mechanical calculations using Gaussian basis sets, as implemented within the program GAUSSIAN-09.[61] The X-ray determined geometries of all the complexes were first relaxed in vacuum using the B3LYP functional,[62,63] the

(57) Soler, J. M.; Artacho, E.; Gale, J. D.; Garcia, A.; Junquera, J.; Ordejon, P.; Sanchez-Portal, D. *J. Phys.: Condens. Matter* **2002**, *14*, 2745.
(58) Armiento, R.; Mattsson, A. E. *Phys. Rev. B* **2005**, *72*, 085108.
(59) Troullier, N.; Martins, J. L. *Phys. Rev. B* **1991**, *43*, 1993.
(60) Junquera, J.; Paz, O.; Sanchez-Portal, D.; Artacho, E. *Phys. Rev. B* **2001**, *64*, 235111.
(61) Frisch, M. J.; Trucks, G. W.; Schlegel, H. B.; Scuseria, G. E.; Robb, M. A.; Cheeseman, J. R.; Scalmani, G.; Barone, V.; Mennucci, B.; Patersson, G. A.; Nakatsuji, H.; Caricato, M.; Li, X.; Hratchian, H. P.; Izmaylov, A. F.; Bloino, J.; Zheng, G.; Sonnengerg, J. L.; Hada, M.; Ehara, M.; Toyota, K.; Fukuda, R.; Hasegawa, J.; Ishida, M.; Nakajima, T.; Honda, Y.; Kitao, O.; Nakai, H.; Vreven, T.; Montgomery, J., J. A.; Peralta, J. E.; Ogliaro, F.; Bearpark, M.; Heyd, J. J.; Brothers, E.; Kudin, K. N.; Staroverov, V. N.; Kobayashi, R.; Normand, J.; Raghavachari, K.; Rendell, A.; Burant, J. C.; Iyengar, S. S.; Tomasi, J.; Cossi, M.; Rega, N.; Millam, J. M.; Klene, M.; Knox, J. E.; Cross, J. B.; Bakken, V.; Adamo, C.; Jaramillo, J.; Gomperts, R.; Stratmann, R. E.; Yazyev, O.; Austin, A. J.; Cammi, R.; Pomelli, C.; Ochterski, J. W.; Martin, R. L.; Morokuma, K.; Zakrzewski, V. G.; Voth, G. A.; Salvador, P.; Dannenberg, J. J.; Dapprich, S.; Daniels, A. D.; Farkas, O.; Foresman, J. B.; Ortiz, J. V.; Cioslowski, J.; Fox, D. J. *Gaussian 09*, Revision A.02; Wallingford, CT, 2009.
(62) Becke, A. D. *J. Chem. Phys.* **1993**, *98*, 5648.
(63) Lee, C.; Yang, W.; Bard, A. J. *Phys. Rev. B* **1988**, *37*, 785.

Stuttgart-Dresden (SDD) Effective Core Potential[64] for the Re atoms, and the 6-31G** basis set for the C, H, N, and O atoms. The ground state structures were then reoptimized in the presence of the PCM solvation model[65] with parameters set appropriate to mimic dichloromethane as a medium. To check the convergence of the calculations with respect to the basis set, the final geometries were reoptimized in dichloromethane with the 6-311G** basis set. In the latter case, no significant differences have been observed in the geometries (atomic rmsd < 0.02 Å). The electronic absorption spectra for the singlet−singlet transitions were then computed using Time-Dependent Density Functional Theory (TDDFT) at the B3LYP/6-311++G**//B3LYP/6-311G** level again in the presence of the PCM continuum solvent model. The nine lowest lying excitation energies were determined in all cases, except for one ligand (**Tph**), where an additional three transitions were computed to locate the strong transition at the lower bound of the observed experimental spectrum.

Results and Discussion

Synthesis of the Complexes. The four tetrazole ligands used in this work were prepared by addition of NaN_3 to the corresponding nitrile in toluene and in the presence of triethylammonium chloride, using a method reported by Koguro and co-workers.[51] The cationic precursor *fac*-[Re(**N^N**)(CO)$_3$(NCCH$_3$)][BF$_4$] was prepared following previously published procedures:[55] [Re(CO)$_5$Cl] was first treated with the corresponding diimine to displace two carbonyl ligands, followed by chloride extraction with $AgBF_4$ in refluxing acetonitrile. *fac*-[Re(**N^N**)(CO)$_3$(NCCH$_3$)][BF$_4$] was finally reacted with the corresponding tetrazole ligand in the presence of triethylamine in refluxing acetonitrile to yield the desired products. Following this procedure (Figure 1) we were able to obtain all the Re complexes in moderate to good yields. The chloride extraction reaction was always performed by strictly using 1 equiv of $AgBF_4$ with respect to *fac*-[Re(**N^N**)(CO)$_3$Cl]. If an excess of silver salt was used, we noticed the formation of an off-white precipitate when the cationic precursor was then reacted with the tetrazole ligand and the triethylamine base. In this case the yield of the final Re complexes was significantly lowered. This unwanted byproduct was light sensitive as its color darkened upon prolonged exposure to light. Its IR spectrum was very similar to that of the tetrazolate ligand; hence, we concluded that the precipitate was mainly composed of silver tetrazole salts. Using a 1:1 stoichiometric ratio between $AgBF_4$ and the Re precursor avoided the formation of the byproduct and improved the overall yields.

Although the complexes have a similar chemical structure, with small variations only in the nature of the diimine ligand **N^N** and the *para* substituent on the aryltetrazolato ligand, their solubilities are quite different. The majority of the complexes are in fact fairly insoluble, some of them, namely, *fac*-[Re(**bipy**)(CO)$_3$(**Tbdz**)], *fac*-[Re(**bipy**)(CO)$_3$(**Tacy**)], *fac*-[Re(**phen**)(CO)$_3$(**Tacy**)], and *fac*-[Re(**bipy**)(CO)$_3$(**Tmeb**)], are not completely soluble even in hot DMSO. On the other hand, the three complexes *fac*-[Re(**bipy**)(CO)$_3$(**Tph**)], *fac*-[Re(**phen**)(CO)$_3$(**Tph**)], and *fac*-[Re(**phen**)(CO)$_3$(**Tbdz**)] are soluble in acetonitrile, chlorinated and more polar solvents such as DMSO. Therefore, the specific solubility of each compound determined the purification method used, with the more soluble complexes isolated via alumina filled column chromatography. Generally, three yellow fractions were obtained: (i) the first fraction eluted with a CH_2Cl_2/CH_3CN 8:2 mixture, always present in very low amount, was identified as the previously unreacted *fac*-[Re(**N^N**)(CO)$_3$Cl] from the halogen extraction reaction; (ii) the second fraction eluted with a CH_2Cl_2/CH_3CN 4:6 mixture corresponded to the targeted tetrazolato complex; (iii) the third fraction, eluted with CH_3CN/MeOH 8:2 was not clearly identified and it contained a mixture of Re complexes, with analysis suggesting positively charged species. The more insoluble complexes were purified via filtration from hot acetonitrile to remove dissolved byproducts.

Table 1. Stretching Frequency Values (cm^{-1}) for the Carbonyl Bands of the Prepared Complexes[a]

compound	A′(1)	A′(2)	A″	
fac-[Re(**bipy**)(CO)$_3$Cl]	2013	1891		1872
fac-[Re(**phen**)(CO)$_3$Cl]	2014	1923		1885
fac-[Re(**bipy**)(CO)$_3$(NCCH$_3$)][BF$_4$]	2031		1909[b]	
fac-[Re(**phen**)(CO)$_3$(NCCH$_3$)]$^+$	2040[c]		1938[c]	
fac-[Re(**bipy**)(CO)$_3$(**Tph**)]	2018	1893[b]		
fac-[Re(**phen**)(CO)$_3$(**Tph**)]	2019	1909		1884
fac-[Re(**bipy**)(CO)$_3$(**Tbdz**)]	2021		1885[b]	
fac-[Re(**phen**)(CO)$_3$(**Tbdz**)]	2020	1916		1892
fac-[Re(**bipy**)(CO)$_3$(**Tacy**)]	2017		1898[b]	
fac-[Re(**phen**)(CO)$_3$(**Tacy**)]	2016	1913		1887
fac-[Re(**bipy**)(CO)$_3$(**Tmeb**)]	2020		1902[b]	
fac-[Re(**phen**)(CO)$_3$(**Tmeb**)]	2020	1912		1887

[a] Spectra recorded in solid state. [b] The A′(2) and A″ modes appear as one broad signal. [c] Previously published data obtained from acetonitrile solution.[66]

IR and NMR Spectroscopy. All the synthesized *fac*-[Re(**N^N**)(CO)$_3$(**L**)]-type species display IR spectra consistent both with the facial configuration of the carbonyl ligands and with the C_s symmetry of the complexes, as witnessed by the presence of three intense absorptions which are observed in the 2022 and 1880 cm^{-1} region (Table 1). According to previous reports on similar compounds, the sharp band at higher frequency, about 2020 cm^{-1}, was attributed to the A′(1) mode (totally symmetric in-phase stretching of the three CO ligands), whereas the remaining two bands at intermediate and lower frequencies were assigned to the A′(2) (totally symmetric out-of-phase stretching) and A″ modes (asymmetric stretching of the equatorial CO ligands).[66−69] As sometimes observed in *fac*-[Re(**N^N**)(CO)$_3$(**L**)]-type complexes, in the case **N^N** = **bipy**, the A′(2) and A″ bands are superimposed into a single broad band.[34,66,70] The relative frequencies of the carbonyl peaks are consistent with the neutral nature of the complexes. The values are lowered with respect to their corresponding cationic precursors,[66] confirming an increase in electron

(64) Andrae, D.; Haussermann, U.; Dolg, M.; Stoll, H.; Preuss, H. *Theor. Chim. Acta* **1990**, *77*, 123.
(65) Tomasi, J.; Mennucci, B.; Cammi, R. *Chem. Rev.* **2005**, *105*, 2999.
(66) Bullock, J. P.; Carter, E.; Johnson, R.; Kennedy, A. T.; Key, S. E.; Kraft, B. J.; Saxon, D.; Underwood, P. *Inorg. Chem.* **2008**, *47*, 7880.
(67) Vlcek, A. *Top. Organomet. Chem.* **2010**, *29*, 73.
(68) Dattelbaum, D. M.; Omberg, K. M.; Schoonover, J. R.; Martin, R. L.; Meyer, T. J. *Inorg. Chem.* **2002**, *41*, 6071.
(69) Dattelbaum, D. M.; Martin, R. L.; Schoonover, J. R.; Meyer, T. J. *J. Phys. Chem. A* **2004**, *108*, 3518.
(70) Bredenbeck, J.; Helbing, J.; Hamm, P. *J. Am. Chem. Soc.* **2004**, *126*, 990.

Table 2. NMR Chemical Shift Data (ppm, DMSO-d_6) Relative to H_o, H_m, C_5 for the Tetrazole Ligands and the Re Complexes

	Re complexes			corresponding 5-aryl-1*H*-tetrazole		
compound	δH_o	δH_m	δC_5	δH_o	δH_m	δC_5
fac-[Re(**bipy**)$(CO)_3$(**Tph**)]	7.67−7.65[a]	7.36−7.32[a,b]	162.3	8.05−8.03[a]	7.61−7.58[a,b]	155.2
fac-[Re(**phen**)$(CO)_3$(**Tph**)]	7.51−7.48[a]	7.26−7.24[a,b]	162.1			
fac-[Re(**phen**)$(CO)_3$(**Tbdz**)]	7.73	7.82	161.5	8.25	8.11	155.5
fac-[Re(**phen**)$(CO)_3$(**Tmeb**)]	7.66	7.87	161.5	8.17	8.13	155.3

[a] Multiplet range. [b] The peak includes the resonances of H_m and H_p.

density for the Re centers when the anionic tetrazolato ligand displaces the coordinated acetonitrile molecule. When compared with the parent neutral *fac*-[Re(**N^N**)$(CO)_3$Cl] complexes, a slight increase in the carbonyl frequencies is observed. The increment was ascribed to the π accepting nature of the tetrazole ring, which in turn causes a slight decrease of electron density around the Re center upon backbonding involving the 5d(Re) and the π*(tetrazole) orbitals. Although aryltetrazolato ligands coordinated to $[FeCp(CO)_2]^+$ fragments evidenced a strong π-accepting character,[49,71] the metal to ligand backbonding interaction seems to be somewhat reduced for the Re complexes investigated within this work. This effect might be explained by considering the less favorable overlap of 5d(Re) orbitals with 2p(N) orbitals rather than 3d(Fe) with 2p(N).

^{1}H and ^{13}C NMR data were obtained from deuterated DMSO solutions. The number of peaks, chemical shifts, and integration values for each spectrum are consistent with the proposed formulation of the complexes, namely, *fac*-[Re(**bipy**)$(CO)_3$(**Tph**)], *fac*-[Re(**phen**)$(CO)_3$(**Tph**)], *fac*-[Re(**phen**)$(CO)_3$(**Tbdz**)], and *fac*-[Re(**phen**)$(CO)_3$(**Tmeb**)]. On the other hand, it was not possible to obtain accurate NMR data for the remaining complexes because of their lower solubility. Table 2 reports the chemical shift values for H_o, H_m, and C_5 of the phenyl and tetrazole rings respectively (see Figure 2 for a referencing scheme relative to the NMR assignment). Two sets of data were collected: the first on the 5-aryl-1*H*-tetrazole species and the second after their coordination to the Re center. In the case of **Tph**H, *fac*-[Re(**bipy**)$(CO)_3$(**Tph**)], and *fac*-[Re(**phen**)$(CO)_3$(**Tph**)] the chemical shift values of H_o and H_m can be easily assigned taking into consideration the deshielding effect caused by the tetrazole ring and the lack of an electron withdrawing group in the *para* position. For the other species the chemical shifts of the H_o and H_m were assigned by analyzing also the 1D NOE (only for **Tbdz**H and *fac*-[Re(**phen**)$(CO)_3$(**Tbdz**)]) and HMBC spectra. As it can be seen from the values in Table 2, in each case there is a slight shielding effect on both H_o and H_m upon coordination of the aryltetrazolato ligand to the Re center. Moreover, the H_o in *fac*-[Re(**phen**)$(CO)_3$(**Tbdz**)] and *fac*-[Re(**phen**)$(CO)_3$(**Tmeb**)] is found to be more shielded with respect to H_m, a situation which is reversed compared to the parent 5-aryl-1*H*-tetrazole species. On the other hand, the chemical shift of the C_5 in the complexes is deshielded of about 6−7 ppm after coordination. The deshielding of the H_o and H_m and the shielding of C_5 in the 5-aryl-1*H*-tetrazole molecules are mainly caused by the inductive electron withdrawing nature (−I) of the

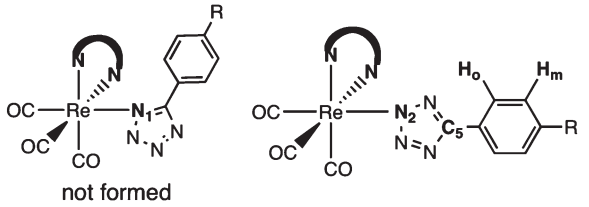

Figure 2. Representation of the N1 and N2 coordinated linkage isomers, with the latter also reporting the NMR assigment scheme.

tetrazole ring. The comparison of the two sets of data evidences the presence of a stronger mesomeric electron donating effect (+M) of the tetrazole ring in the complexes, which is also consistent with an extended interannular conjugation. This conjugation suggests coplanarity between the two rings as previously shown by the studies of Butler and co-workers.[72,73] In the case of the parent 5-aryl-1*H*-tetrazole species, the steric hindrance caused by the N1−H and the adjacent phenyl C−H bond favors the rotation of the phenyl ring with respect to the tetrazole one, therefore diminishing the conjugation and hence the intensity of the +M donation, thus resulting in a predominant −I effect. Therefore, the NMR data also support that the coordination of the Re center to the tetrazole ring is regioselective for the N2 position.[49,71,74,75]

All of the complexes show in their ^{13}C NMR spectra two close peaks belonging to the three carbonyl ligands in the 198−194 ppm region. This inequivalence was ascribed to the two different N-donor ligands (bidentate diimine and tetrazolato) in *trans* to the carbonyl ones, consistently with a C_s point group.

X-ray Structural Investigation. Single crystals of all the prepared compounds were grown from hot saturated DMSO solutions. The most insoluble complexes were heated in a DMSO solution (≈160 °C) and any undissolved solid was immediately filtered through Celite. The clear solution was then left to cool down undisturbed to room temperature. If after a couple of days no crystals appeared, the whole process was started again by reheating the solution. We used this crystallization method also for the more soluble complexes, as layering the corresponding dichloromethane solutions with hexane or diethylether yielded crystals of poorer X-ray diffraction quality. The structures of the Re complexes are shown in Figures 3−6. All the structures contain one individual complex per asymmetric unit, with the exception of

(71) Palazzi, A.; Stagni, S.; Selva, S.; Monari, M. *J. Organomet. Chem.* **2003**, *672*, 130.

(72) Butler, R. N.; Garvin, V. C.; Lumbroso, H.; Liegeois, C. *J. Chem. Soc., Perkin Trans. 2* **1984**, 721.

(73) Butler, R. N.; Garvin, V. C. *J. Chem. Soc., Perkin Trans. 1* **1981**, 390.

(74) Butler, R. N.; McEvoy, T. M. *J. Chem. Soc., Perkin Trans. 2* **1978**, 1087.

(75) Palazzi, A.; Stagni, S. *J. Organomet. Chem.* **2005**, *690*, 2052.

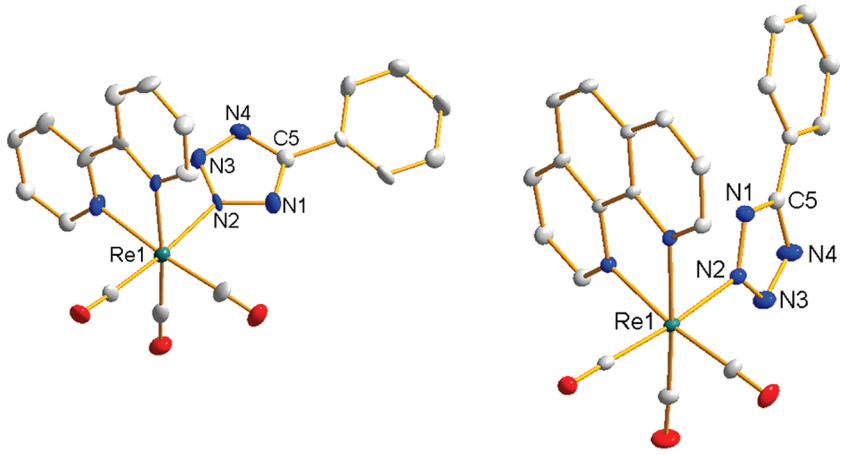

Figure 3. X-ray crystal structure of *fac*-[Re(**bipy**)$(CO)_3$(**Tph**)] (left) and *fac*-[Re(**phen**)$(CO)_3$(**Tph**)] (right) where thermal ellipsoids have been drawn at the 50% probability level. Hydrogen atoms are omitted for clarity.

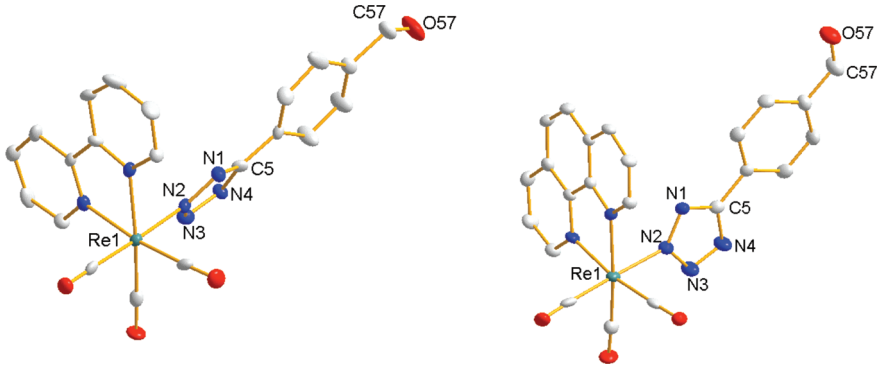

Figure 4. X-ray crystal structure of *fac*-[Re(**bipy**)$(CO)_3$(**Tbdz**)] (left) and *fac*-[Re(**phen**)$(CO)_3$(**Tbdz**)] (right) where thermal ellipsoids have been drawn at the 30% and 50% probability level respectively. Hydrogen atoms are omitted for clarity.

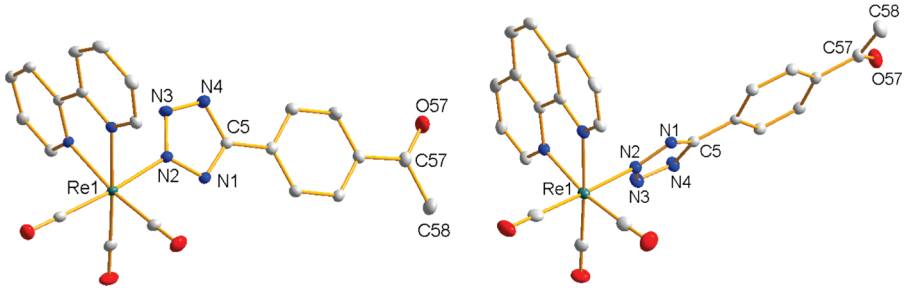

Figure 5. X-ray crystal structure of *fac*-[Re(**bipy**)$(CO)_3$(**Tacy**)] (left) and *fac*-[Re(**phen**)$(CO)_3$(**Tacy**)] (right) where thermal ellipsoids have been drawn at the 50% probability level. Hydrogen atoms are omitted for clarity.

fac-[Re(**phen**)$(CO)_3$(**Tmeb**)] (Figure 6), which contains two crystallographically independent complexes per asymmetric unit. In this case, the two complexes are approximately related by a cell translation of 0.5 Å along the direction of the *a* axis, as shown in the cell projection in Figure 7. The two complexes are similar with differences confined to minor rotations of the ligands. The angles between the plane of the **phen** and the tetrazole rings are 104.1(2)° and 103.2(2)° with those between the phenyl and tetrazole rings being 9.1(2) ° and 10.1(2)° for molecules 1 and 2, respectively.

The analysis of the structural data further confirms, along with the ^{1}H and ^{13}C NMR results, that the coordination of the Re center is regioselective for the N2 position of the tetrazole ring (Figure 2). This evidence also suggests that neither in solution nor in the solid state is the N1 linkage isomer formed. This can be ascribed to a combination of steric bulkiness of both the *fac*-[Re(**N^N**)$(CO)_3]^+$ fragment and the benzene ring attached to the tetrazole.

The extent of intermolecular interaction throughout the lattice varies within each structure, with the observed general trend that complexes bearing **phen** have a higher tendency in favoring π interaction. Both *fac*-[Re(**phen**)$(CO)_3$(**Tph**)] and *fac*-[Re(**phen**)$(CO)_3$(**Tbdz**)] are arranged to maximize π stacking between the **phen** units, with an average distance of 3.5 Å. On the other hand, in both *fac*-[Re(**phen**)$(CO)_3$(**Tacy**)] and *fac*-[Re(**phen**)$(CO)_3$(**Tmeb**)] there is evidence of π stacking between the tetrazolato ligands and the **phen** units ($\approx$ 3.5 Å between the diimine

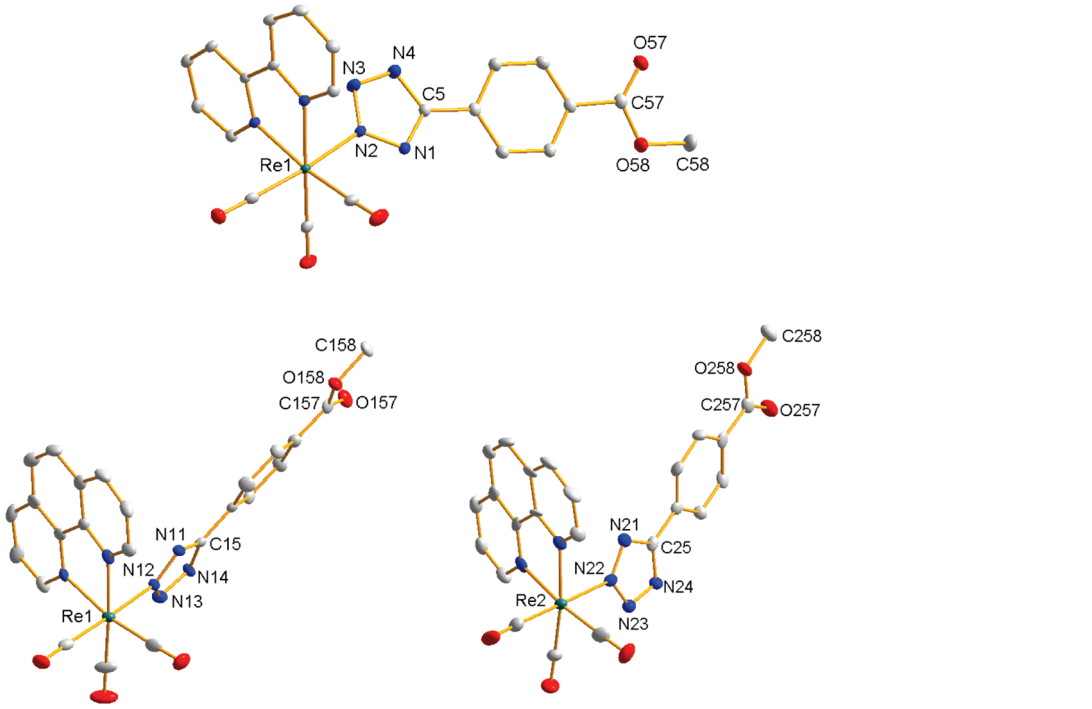

Figure 6. X-ray crystal structure of *fac*-[Re(**bipy**)$(CO)_3$(**Tmeb**)] (top) and *fac*-[Re(**phen**)$(CO)_3$(**Tmeb**)] (bottom) where thermal ellipsoids have been drawn at the 50% probability level. Hydrogen atoms are omitted for clarity.

and aryltetrazolato phenyl rings). Only *fac*-[Re(**bipy**)-$(CO)_3$(**Tacy**)] favors stacking between neighboring tetrazolato ligands instead of the **bipy** units, again with an average distance between the two planes of about 3.5 Å. Finally, *fac*-[Re(**bipy**)$(CO)_3$(**Tph**)], *fac*-[Re(**bipy**)$(CO)_3$(**Tbdz**)], and *fac*-[Re(**bipy**)$(CO)_3$(**Tmeb**)] do not exhibit any evidence of π stacking in the lattice. A correlation between the interannular torsion (aryl and tetrazole rings) and the intramolecular interaction seems to indicate that a higher degree of rotation is present (dihedral angle values between 13° and 24°) when there is no evidence of π stacking within the lattice.

Computational Investigation of the Tetrazole and Phenyl Rings Co-planarity. Previous studies on metal complexes bearing 5-aryltetrazolato ligands highlighted a correlation between N2 coordination, extended interannular conjugation, and the coplanar arrangement of the tetrazole and phenyl rings.[49,75] This correlation was obtained by direct comparison of the ^{1}H and ^{13}C NMR data with solid-state structural determinations. While in our study both the spectroscopic and the X-ray diffraction measurements confirm the regioselective N2 coordination, the solid-state structures reveal in some cases a significant degree of rotation between the two rings, as summarized in Table 3. It cannot be excluded that in solution at room temperature the torsional angle is in fact averaged to a more coplanar configuration. Therefore we performed theoretical calculations to predict the relative arrangement of the two rings in solution, as the information is important for the interpretation of the photophysical behavior of the complexes from solution data (see below).

For the case of *fac*-[Re(**bipy**)$(CO)_3$(**Tph**)] the interplay between crystal packing forces and the dihedral angle between the aryl and tetrazole rings has been investigated through quantum mechanical calculations. For the

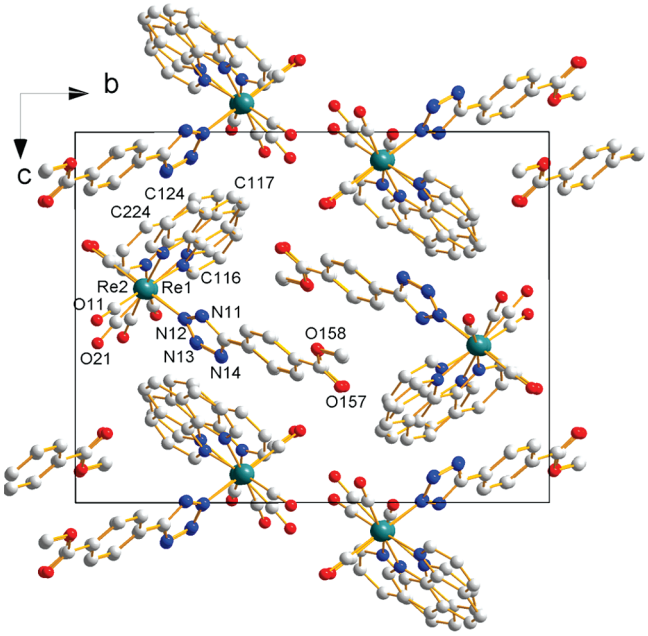

Figure 7. Unit cell content of *fac*-[Re(**phen**)$(CO)_3$(**Tmeb**)] as viewed along the *a* axis.

solid-state material the structure was optimized within the constraint of the crystallographically determined unit cell. For complex condensed phases, the most readily applicable form of quantum mechanics is density functional theory, as has been used in the present work. However, a known limitation of most functionals is the absence of long-range attraction due to van der Waal's forces. While this can be overcome through the use of either empirical corrections,[76] through explicitly adding

(76) Grimme, S. *J. Comput. Chem.* **2004**, *25*, 1463.

Table 3. Dihedral Angle Values between the Tetrazole and the Phenyl Rings As Obtained from X-ray Diffraction Data for the Re Complexes

compound	dihedral angle (deg)
fac-[Re(**bipy**)(CO)$_3$(**Tph**)]	20.37
fac-[Re(**phen**)(CO)$_3$(**Tph**)]	3.26
fac-[Re(**bipy**)(CO)$_3$(**Tbdz**)]	23.51
fac-[Re(**phen**)(CO)$_3$(**Tbdz**)]	1.41
fac-[Re(**bipy**)(CO)$_3$(**Tacy**)]	1.81
fac-[Re(**phen**)(CO)$_3$(**Tacy**)]	12.64
fac-[Re(**bipy**)(CO)$_3$(**Tmeb**)]	13.17
fac-[Re(**phen**)(CO)$_3$(**Tmeb**)]	10.62

on damped dispersion interactions, or via the use of nonlocal functionals designed to reproduce van der Waal's interactions in particular cases,[77] both approaches will introduce greater inaccuracy than using the known unit cell.

After optimization, the calculated acute dihedral angles between the aryl and tetrazole rings in the crystal were found to be 24.6 and 28.2° (the presence of two distinct values is due to the asymmetry of the tetrazole environment). These values compare to 20.4 and 26.8° in the experimental structure, and thus the calculated dihedral angles are slightly higher on average and with a reduced splitting between the two angles. However, there is qualitative agreement in the behavior, in that there is a twisting of the phenyl group with respect to the plane of the tetrazole in the crystal structure.

In the calculations it is now possible to begin to explore the influence of intermolecular forces on this dihedral angle. First of all we reduce the contents of the unit cell to contain only a single molecule, such that the only interactions are with its own image. Because of the anisotropic nature of the unit cell, the images are well separated in the *c* direction, while there remains some weak interaction in the remaining two crystallographic directions. With this transformation the dihedral angles are already substantially reduced to 5.3 and 6.1°. By doubling the unit cell dimensions in the *ab* plane, to further reduce the intermolecular interactions, the dihedral angles are now decreased to 0.2 and 1.4°. A clear trend is apparent that as the intermolecular interactions decrease, so the torsional angles are tending to values close to zero and thus the aryl and tetrazole rings are becoming coplanar to maximize the degree of conjugation.

Photophysical Investigation. The absorption and emission data for the complexes are summarized in Table 4. The absorption profiles (Figure 8) are very similar for all of the complexes, with strong intraligand (IL) $\pi-\pi^*$ absorption bands in the high energy UV (250−310 nm) and in the low energy UV region (350−370 nm), and tailing into the visible region, a mix of weaker ligand-to-ligand charge-transfer (LLCT, tetrazolato to diimine) and MLCT (Re to diimine) bands. The close proximity of LLCT and MLCT "states" has previously been described as one-electron excitations that mix to give rise to a MLLCT state,[67,78−81] especially when strong donor ancillary ligands, such as isocyanides, were incorporated into the [Re(**N^N**)(CO)$_3$]$^+$ coordination sphere. The MLLCT transitions were found to generate very broad low energy absorption bands, as found in the present work.[23,24] The distinction between the IL and the MLLCT nature of the transition was also confirmed by the solvatochromic nature of the latter, for which a greater electric dipole change is associated with the electronic transition. A hypsochromic shift of about $\Delta\lambda$ = 15−20 nm was recorded for the complexes on passing from dichloromethane to DMSO solutions (negative solvatochromism). On the other hand, the transitions assigned to IL $\pi-\pi^*$ were found to be almost insensitive to the solvent change, as expected for transitions associated with a minimal electric dipole change.

Although the molar absorptivities of the MLLCT bands of the complexes are of the same order of magnitude, those bands incorporating **phen** have about 50% higher values as compared to those containing **bipy**. Differences in molar absorptivity have previously been noted in *fac*-[Re(**N^N**)(CO)$_3$L]$^+$ complexes of **bipy** and **phen**, albeit to a lesser extent (10%).[82,83] The main general difference in the λ_{ex} and λ_{em} values (Table 4) arises from the systematically lower absorption and emission energies of the complexes that contain the **bipy** ligand. As the LUMO level is mainly localized on the diimine **N^N** ligand for all the complexes (see below), this effect is counterintuitive to the typically lower π^* levels of **phen** as compared to **bipy**. A similar trend has been noted with increasing donor strength in ancillary ligands connected to the [Re(**N^N**)(CO)$_3$]$^+$ core.[21] As the **N^N** ligand is the primary contributor to the LUMO level, this red-shift is found in both the absorption and the emission bands of the complexes.

The broad and featureless ^{3}MLLCT emission bands are found between 566 and 578 nm (Figure 8 insets). In general, as it can be seen from the values of τ and Φ in Table 4, the complexes *fac*-[Re(**phen**)(CO)$_3$(**L**)] show significantly longer excited state lifetimes and greater quantum yields compared to the analogous *fac*-[Re(**bipy**)(CO)$_3$(**L**)]. The longer excited state lifetimes and quantum yields are associated with the presence of the more rigid **phen** ligands.[82] In all cases, monoexponential decays were observed and excitation spectra of the compounds were similar to the absorption spectra, showing the same broad MLLCT band.

The aryltetrazolato ligands offer the ability to fine-tune the absorption and emission energies of the complexes, and consequently the photophysical performance in terms of lifetime τ and quantum yield Φ, by way of their substituents. The electron-donating or withdrawing capacity of the *para* aryltetrazole R group will influence the energy of any LLCT directly, and indirectly the energy of the MLCT via the Re 5d orbitals. In this study, the presence of EWGs lowers the energy of the HOMO, thus blue-shifting the MLLCT. The effect, albeit very subtle in some cases (e.g., compare the absorption wavelength of *fac*-[Re(**bipy**)(CO)$_3$(**Tph**)] at 370 nm and *fac*-[Re(**bipy**)(CO)$_3$(**Tbdz**)] at 367 nm), is also supported by quantum

(77) Dion, M.; Rydberg, H.; Schroeder, E.; Langreth, D. C.; Lundqvist, B. I. *Phys. Rev. Lett.* **2004**, *92*, 246401.
(78) Vlcek, A.; Zalis, S. *Coord. Chem. Rev.* **2007**, *251*, 258.
(79) Vlcek, A.; Zalis, S. *J. Phys. Chem. A* **2005**, *109*, 2991.
(80) Zalis, S.; Ben Amor, N.; Daniel, C. *Inorg. Chem.* **2004**, *43*, 7978.
(81) Gabrielsson, A.; Busby, M.; Matousek, P.; Towrie, M.; Hevia, E.; Cuesta, L.; Perez, J.; Zalis, S.; Vlcek, A. *Inorg. Chem.* **2006**, *45*, 9789.
(82) Juris, A.; Balzani, V.; Barigelletti, F.; Campagna, S.; Belser, P.; von Zelewsky, A. *Coord. Chem. Rev.* **1988**, *84*, 85.
(83) Kalyanasundaram, K. *J. Chem. Soc., Faraday Trans. 2* **1986**, *82*, 2401.

Table 4. Photophysical Properties of the Re Complexes in Deoxygenated Dichloromethane at Room Temperature[a]

	absorption	emission		
compound	λ_{ex} (ε) nm (cm^{-1} M^{-1})	λ_{em} nm	τ ns	Φ^b (± 15%)
fac-[Re(**bipy**)$(CO)_3$Cl][c]	385(3650)	600	51	0.005
fac-[Re(**phen**)$(CO)_3$Cl][d]	380(4000)	577	300	(0.036)[e]
fac-[Re(**bipy**)$(CO)_3(NCCH_3)$][c]	343(4250)	526	1201	0.41
fac-[Re(**bipy**)$(CO)_3$(**Tph**)]	370(2900)	578	102	0.012
fac-[Re(**phen**)$(CO)_3$(**Tph**)]	358(4250)	571	740	0.054
fac-[Re(**bipy**)$(CO)_3$(**Tbdz**)]	367(3050)	574	130	0.018
fac-[Re(**phen**)$(CO)_3$(**Tbdz**)]	357(4950)	566	945	0.099
fac-[Re(**bipy**)$(CO)_3$(**Tacy**)]	367(3050)	574	119	0.017
fac-[Re(**phen**)$(CO)_3$(**Tacy**)]	357(5350)	566	955	0.097
fac-[Re(**bipy**)$(CO)_3$(**Tmeb**)]	367(2250)[f]	574	122	0.016
fac-[Re(**phen**)$(CO)_3$(**Tmeb**)]	357(5200)	569	923	0.079

[a] The excitation wavelength for the emission spectra corresponds to the maximum absorption of the MLLCT band. The excitation wavelength for the lifetime measurements corresponds to 405 nm, whereas for the quantum yield corresponds to 355 nm. [b] Quantum yields were measured by the dilute solution method using an aerated *fac*-[Re(**bipy**)$(CO)_3(NCCH_3)$][PF_6] solution as reference. [c] Previously published data except for emission maximum.[33] [d] Previously published data.[21] [e] Literature value, measured in degassed benzene.[21] [f] As the complex is strongly insoluble, the ε value is probably underestimated.

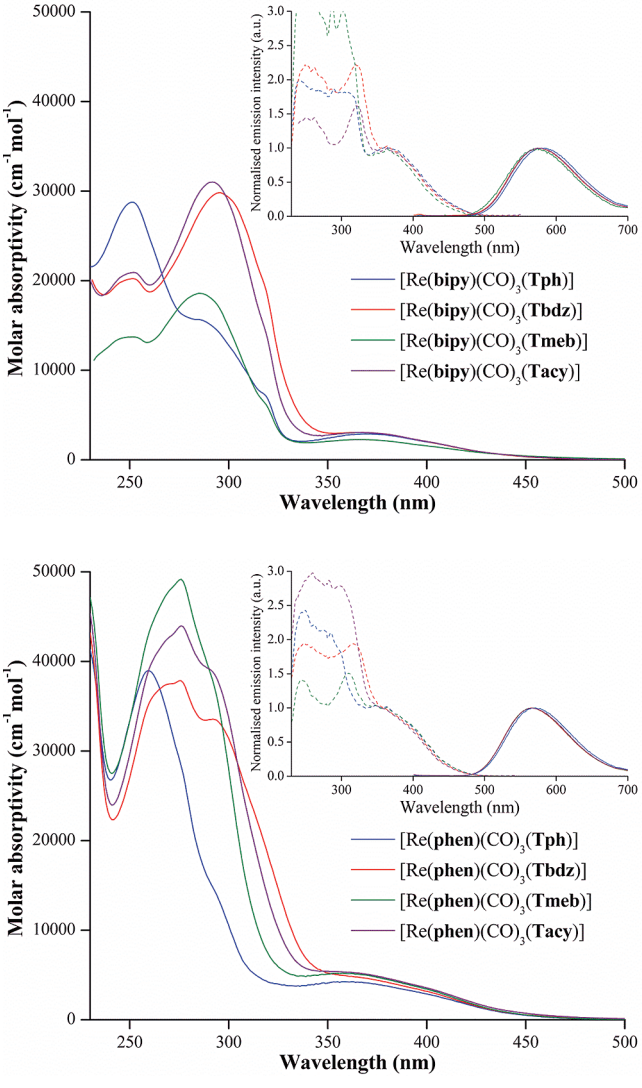

Figure 8. Absorption, emission (inset, full line) and excitation (inset, dotted line) profiles for the *fac*-[Re(N^N)$(CO)_3$(**L**)] complexes in deoxygenated dichloromethane; excitation wavelengths for the emission spectra correspond to the reported absorption maximum of the MLLCT transition of each compound as found in Table 4.

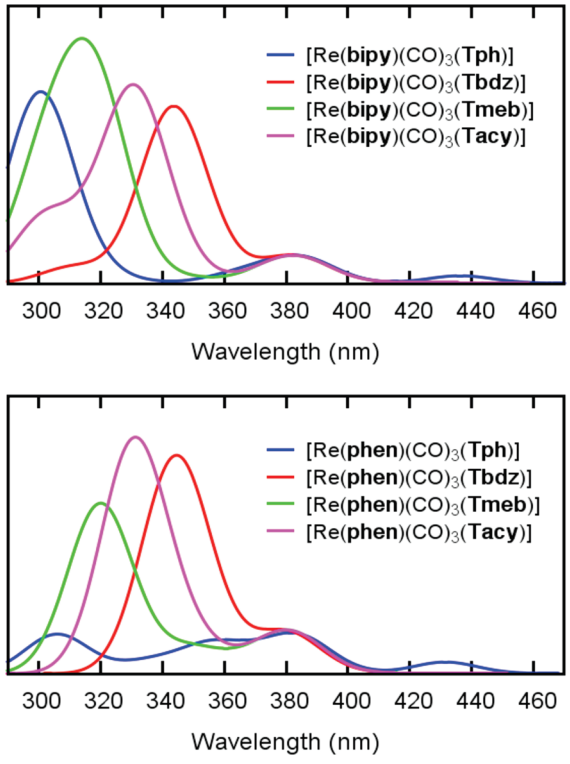

Figure 9. Computed absorption spectra using TDDFT for the singlet−singlet transitions of the *fac*-[Re(N^N)$(CO)_3$(**L**)] complexes in dichloromethane. Intensities are taken from the results of the calculations, while Gaussian broadening is applied using an exponent of 0.005 nm^{-2}.

mechanical calculations (see next section). As a result of the (slight) blue-shift of the emissions for complexes coordinated with aryltetrazolato ligands bearing an EWG, the values of both τ and Φ are increased in accordance with the energy gap law.[34] By comparing the photophysical data of the prepared complexes *fac*-[Re(N^N)$(CO)_3$(**L**)] with *fac*-[Re(N^N)$(CO)_3$Cl] and *fac*-[Re(**bipy**)$(CO)_3(NCCH_3)$][PF_6],[34] the complexes bearing the aryltetrazolato ligands show strong similarities with the neutral ones coordinated to the Cl^- ligand. The blue-shifted absorption and emission energies, as well as the increased lifetimes

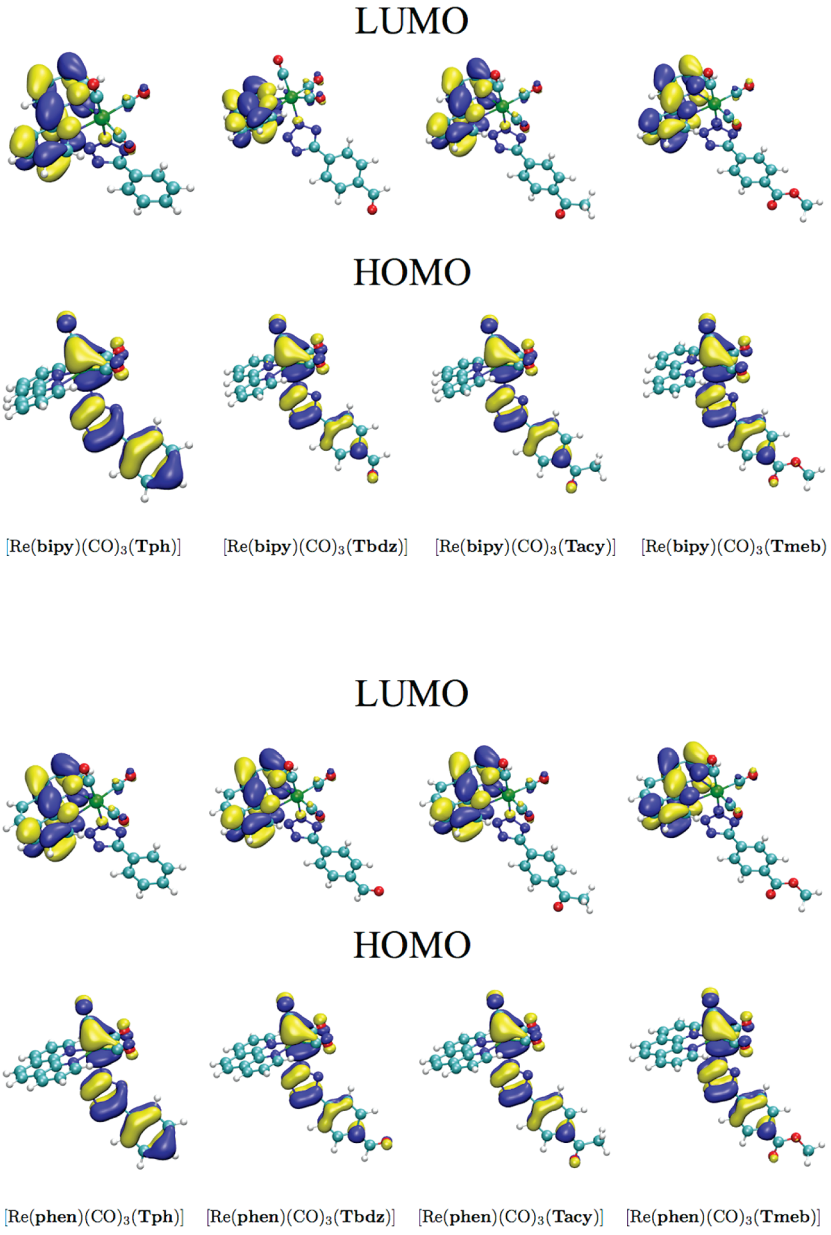

Figure 10. Localization of the HOMO and LUMO orbitals for the four *fac*-[Re(**bipy**)(CO)$_3$(**L**)] (top) and *fac*-[Re(**phen**)(CO)$_3$(**L**)] complexes (bottom).

and quantum yields, are accounted for by the π-accepting nature (albeit not of very strong intensity as confirmed by the IR data) of the tetrazole ring compared with the π-donating nature of the Cl^- ligand. The latter destabilizes the metal orbitals with consequent reduction of the HOMO−LUMO gap and increased k_{nr}. However, other effects, such as the flexibility of the aryl-tetrazolato ligand, might need to be taken into consideration when comparing analogous complexes bearing ancillary ligands of a different nature.

Calculated Absorption Spectrum. To confirm the interpretation of the photophysical results we have performed time-dependent density functional theory calculations to determine the energetics and absorption spectra of the complexes. Although all the complexes display a perfectly planar geometry, we note that different rotations of the aryltetrazolato ligand, with respect to the diimine N^N ligand (Supporting Information, Figure S1), generate almost iso-energetic stable configurations (within 0.01 eV). These configurations have slightly shifted electronic transitions, and often quite different intensites. To allow for this, the absorption spectra have been calculated using the Boltzmann-weighted average over the configurations, with Gaussian broadening of the peaks (Figure 9). The relative energies of the different conformations, as well as the peak positions and intensities are given in full for each complex in the Supporting Information.

The overall appearance of the computed absorption spectrum agrees well with the experimental data. In particular, the order of strong absorption maxima in the range 300−360 nm is consistent with the experimental data. All complexes exhibit a similar weak absorption close to 380 nm, while those of **Tph** have an additional maximum in the region of 430−440 nm. Moreover, the energy trend displayed by the singlet−singlet transitions agrees with the hypothesis that the HOMO−LUMO gap is increased by the presence of an EWG in the *para* position of the aryltetrazolato ligand. Quantitatively,

there are some differences in the precise positions of peaks relative to experiment, which are likely to be a result of both the limitations in the exchange-correlation description employed and also the approximate nature of the solvent model used to describe the surrounding environment of dichloromethane.

Although Kohn−Sham states should be treated with caution, because of the self-interaction error, the HOMO and LUMO provide some useful insight as to the atomic contributions. Here the density functional calculations indicate that for all the complexes in the singlet state the HOMO orbital is mainly localized on the Re center and remarkably delocalized over the entire tetrazole ligand. This delocalization also accounts for the mixing of LLCT and MLCT. On the other hand, the LUMO is localized exclusively on either the **bipy** or the **phen** ligands (Figure 10).

All the relaxed configurations were also excited to a triplet state and reoptimized in dichloromethane with spin unrestricted B3LYP. These calculations confirm that the singlet state is the ground state in all cases, while the singlet−triplet energy difference lies in the range 467−516 nm, placing the transition in the gap as expected. The singlet−triplet energy difference is systematically lower by 10 nm, on average, for phenanthroline as a ligand, which accords with the experimentally observed shift of 5−8 nm.

Conclusions

In this study, the direct synthesis of neutral *fac*-[Re(**N^N**)-$(CO)_3$(**L**)] complexes, where **N^N** is either **bipy** or **phen** and **L** is a *para* functionalized 5-aryltetrazolato ligand, has been investigated. The complexes exist exclusively as the N2 linkage isomer, which allows for maximization of interannular conjugation between the tetrazole and phenyl rings (although some of them show distortion in the solid-state). The spectroscopic investigation has pointed out that the tetrazolato anion is a good σ donor but also a partial π acceptor, thus resulting in a slightly reduced electron density on the metal center compared with the parent *fac*-[Re(**N^N**)-$(CO)_3$X] (X = Cl, Br) complexes. The absorption and emission transitions, in accordance with theoretical calculations, result from a mixing of LLCT and MLCT, which are therefore more properly described as MLLCT. The effect is also visible in the photophysical data, and a trend related to a blue-shift is also evidenced upon addition of EWG onto the aryltetrazolato ligand. Since this blue-shift is the consequence of a wider HOMO−LUMO gap, an improvement of τ and Φ is also noted. However, at the same time these parameters might also be adversely affected by the introduction of the flexible aryltetrazolato ligand. This very last effect is currently under investigation.

Acknowledgment. This work was supported by the Australian Research Council and Curtin University (IRGS-46251). M.M. also wishes to thank the ARC for the APD Fellowship DP0985481. P.R. and J.D.G. thank the ARC for fellowships under Grant DP0986999, as well as NCI and iVEC for provision of computing resources. G.S.H. thanks the Natural Sciences and Engineering Research Council of Canada. A/Prof. Philip C. Andrews and Prof. Peter C. Junk (Monash University) are kindly acknowledged for providing the [$Re(CO)_5Cl$]. M.M., S.M., and S.S. wish to thank Prof. A. Palazzi for helpful discussion on IR spectroscopy. The referees are also acknowledged for providing insightful feedback.

Supporting Information Available: X-ray crystallographic data in CIF format. Full details of the computed singlet−singlet transition energies and oscillator strengths. This material is available free of charge via the Internet at http://pubs.acs.org.